Journal of Medicinal Chemistry

Article

Naphtho[1,2-*d*]isothiazole Acetic Acid Derivatives as a Novel Class of Selective Aldose Reductase Inhibitors

Federico Da Settimo, Giampaolo Primofiore, Concettina La Motta, Stefania Sartini, Sabrina Taliani, Francesca Simorini, Anna Maria Marini, Antonio Lavecchia, Ettore Novellino, and Enrico Boldrini

J. Med. Chem., **2005**, 48 (22), 6897-6907• DOI: 10.1021/jm050382p • Publication Date (Web): 01 October 2005

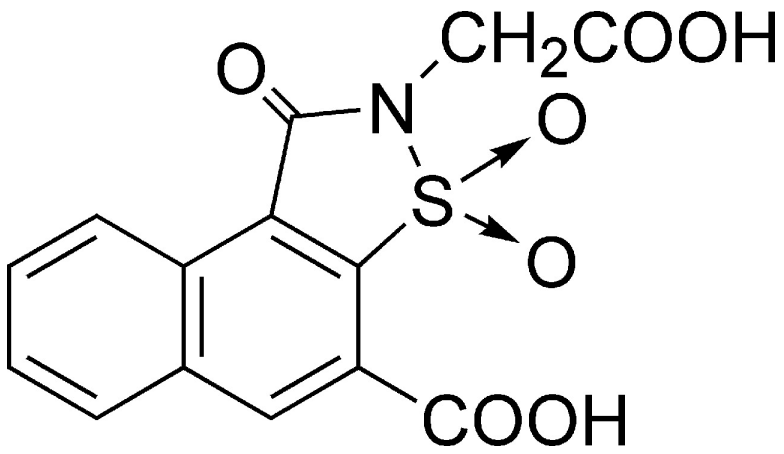

More About This Article

Additional resources and features associated with this article are available within the HTML version:

- Supporting Information
- Links to the 6 articles that cite this article, as of the time of this article download
- Access to high resolution figures
- Links to articles and content related to this article
- Copyright permission to reproduce figures and/or text from this article

View the Full Text HTML

Journal of Medicinal Chemistry is published by the American Chemical Society. 1155 Sixteenth Street N.W., Washington, DC 20036

Naphtho[1,2-*d*]isothiazole Acetic Acid Derivatives as a Novel Class of Selective Aldose Reductase Inhibitors

Federico Da Settimo,[†] Giampaolo Primofiore,[†] Concettina La Motta,*[,†] Stefania Sartini,[†] Sabrina Taliani,[†] Francesca Simorini,[†] Anna Maria Marini,[†] Antonio Lavecchia,[§] Ettore Novellino,[§] and Enrico Boldrini[‡]

Dipartimento di Scienze Farmaceutiche, Università di Pisa, Via Bonanno 6, 56126 Pisa, Italy, Dipartimento di Chimica Farmaceutica e Tossicologica, Università di Napoli "Federico II", Via D. Montesano, 49, 80131 Napoli, Italy, and Opocrin S.p.A., Via Pacinotti 3, 41040 Corlo di Formigine, Modena, Italy

Received April 22, 2005

Acetic acid derivatives of naphtho[1,2-*d*]isothiazole (NiT) were synthesized and tested as novel aldose reductase (ALR2) inhibitors. The parent compound **11** exhibited a fair inhibitory activity ($IC_{50} = 10\ \mu M$), which was enhanced by 2 orders of magnitude by introducing a second carboxylic group at position 4 (**13** and **14**: $IC_{50} = 0.55$ and $0.14\ \mu M$, respectively). Substitution of the acetic acid function with an apolar group gave inactive (**29**) or poorly active (**25**, **26**, **30**) compounds, thus demonstrating that the 2-acetic group is involved in the enzyme pharmacophoric recognition while the 4-carboxylic moiety has only an accessory role. The potent compounds **11**, **13**, **14**, **26** all proved to be selective for ALR2, since none of them inhibited aldehyde reductase, sorbitol dehydrogenase, or glutathione reductase. The isopropyl ester **31**, a prodrug of **14**, was found to be effective in preventing cataract development in severely galactosemic rats, when administered as an eyedrop solution. The theoretical binding mode of **13** and **14**, obtained by docking simulations into the ALR2 crystal structure, was fully consistent with the structure−activity relationships in the NiT series.

Introduction

Diabetes mellitus is a debilitating disease that affects over 200 million people worldwide. It can be successfully controlled by the administration of insulin and/or potent oral hypoglycemics, following newer therapeutic and preventive modalities. Despite these advances in treatment, it still remains the cause of significant morbidity and mortality because of a progressive impairment of the nervous, renal, vascular, and visual systems. Damage of these tissues results from biochemical and functional alterations, occurring in response to a prolonged exposure to hyperglycemia. Many hypotheses have been proposed to explain the pathogenic mechanism leading to these alterations, including impairment of antioxidant defense, nonenzymatic glycation of proteins, and activation of protein kinase C isoforms. The prominent theory suggests that they are causally linked to an increased flux of glucose through the polyol pathway.[1−9]

Aldose reductase (alditol/$NADP^+$ oxidoreductase, EC 1.1.1.21, ALR2) is the first enzyme of the polyol pathway. It catalyzes the NADPH-dependent reduction of glucose to sorbitol, which is then oxidized to fructose by sorbitol dehydrogenase (L-iditol/NAD^+, 5-oxidoreductase, EC 1.1.1.14, SDH). Because ALR2 has a low substrate affinity to glucose, the conversion of glucose to sorbitol is generally nonsignificant in normoglycemic conditions. Actually, ALR2 must compete directly with hexokinase of the glycolytic pathway for the utilization of glucose, and because the substrate affinity of hexokinase is greater than that of ALR2, glucose is preferentially phosphorylated with ATP by this enzyme. Under hyperglycemic conditions, hexokinase is rapidly saturated and the polyol pathway becomes activated. Sorbitol is formed more rapidly than it is converted to fructose, and its polarity hinders its easy penetration through membranes and subsequent removal from tissues by diffusion. The resulting elevated intracellular concentration of sorbitol increases cellular osmolarity, which in turn initiates a cascade of events that result in the development of long-term diabetic complications.

In addition to the osmotic imbalance, the polyol pathway is the major contributor to the generation of hyperglycemic oxidative stress. An increase in the ALR2 activity causes a substantial depletion of its cofactor NADPH, which is also required for glutathione reductase (GR) to regenerate glutathione (GSH). Thus, a significant decrease in the GSH level occurs and the cellular antioxidant capacity is greatly impaired. Also, the oxidation of sorbitol to fructose via SDH results in a decrease in the cytosolic NAD^+/NADH ratio, increasing the amount of NADH that can be utilized by NADH oxidase to generate reactive oxygen species (ROS). Moreover, the increase in fructose levels accelerates the development of diabetic complications, since fructose and its metabolites are more potent nonenzymatic glycation agents than glucose.[10−13] Inhibition of ALR2 is therefore a useful therapeutic strategy to prevent the onset or at least delay the progression and the severity of these complications.

Many compounds have been shown to inhibit the enzyme with various degrees of efficacy and specificity. Currently known ALR2 inhibitors (ARIs) are usually divided into two classes: (i) acetic acid derivatives, like tolrestat, zopolrestat, and epalrestat; (ii) cyclic imides,

* To whom correspondence should be addressed. Phone: (+)39 050 2219 547. Fax: (+)39 050 2219 605. E-mail: lamotta@farm.unipi.it.
[†] Università di Pisa.
[§] Università di Napoli "Federico II".
[‡] Opocrin S.p.A.

10.1021/jm050382p CCC: $30.25
Published on Web 10/01/2005

Chart 1

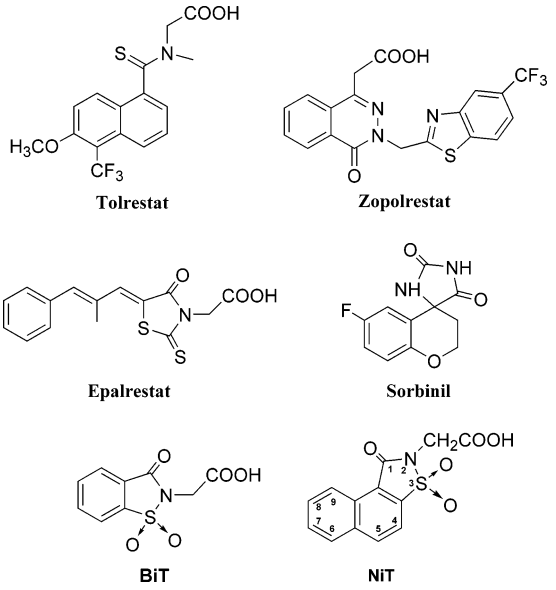

such as sorbinil (Chart 1). Despite being structurally different, they all share common structural requirements, represented by a planar aromatic moiety and an acidic function ionized at the ALR2 active site.[14−18]

Promising products during in vitro studies or in trials with animal models often fail to proceed any further because of a lack of efficacy or because of adverse side effects mainly attributed to pharmacokinetic problems and a lack of specificity for the target enzyme. To date, only epalrestat is successfully marketed for treatment of diabetic neuropathy, in Japan.

ALR2 is closely related to other enzymes, especially aldehyde reductase (ALR1), SDH, and GR. ALR1 is a detoxifying enzyme that belongs to the aldo−keto reductase family, like ALR2. They both exhibit the highest functional and structural homology in the family, showing 51% identity in amino acid sequence between human ALR2 and ALR1.[19] SDH is the second enzyme in the polyol pathway, and under diabetic conditions, its inhibition, although useful to restore the altered cytoplasmic redox state, increases sorbitol levels, thus accelerating cataract formation.[20,21] GR maintains physiological levels of GSH, which in turn prevents glycosylation of protein and protects against oxidative stress. Furthermore, the intracellular accumulation of oxidized glutathione (GSSG), resulting from inhibition of GR, leads to a structural modification of ALR2, which greatly reduces its catalytic efficiency and its sensitivity to ARI action.[22,23] The attention of medicinal chemistry is therefore directed toward the discovery of more specific and clinically effective inhibitors.

Our well-documented interest in the field of carboxylic acid inhibitors[24,25] led us to develop a series of 1,1-dioxide-benzo[*d*]isothiazol-3-one alkanoic acids (BiT) as a novel class of ARIs (Chart 1). These compounds proved to be relatively potent inhibitors, with IC_{50} values in the micromolar range. The 4-NO_2 acetic acid derivative is the most active one, with an IC_{50} of 5.5 μM.[26,27]

It is well-known that the in vitro ALR2 inhibitory efficacy of a compound is a function both of its acidic group ionized at the anion binding site and of its lipophilic scaffold interacting with the enzyme hydrophobic catalytic site, which determine not only the inhibitory potency but also the selectivity of an inhibitor. Thus, an increase in the overall lipophilicity of BiT inhibitors might result in an improvement of the in vitro effectiveness and, possibly, in ALR2 selectivity. For this reason, we decided to insert a fused benzene ring into the benzoisothiazole backbone to obtain the acetic acid derivatives of 3,3-dioxide-1,2-dihydronaphtho[1,2-*d*]-isothiazol-1-one (NiT) as a novel class of ARIs (Chart 1).

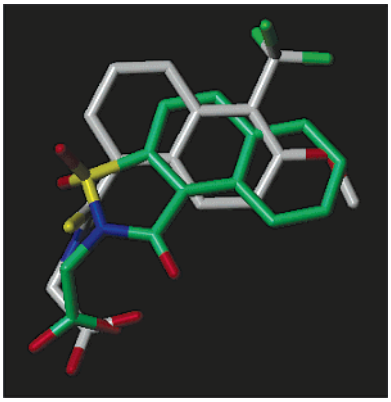

Figure 1. Overlay of inhibitor **11** (green-blue) on the experimentally determined ALR2-bound conformation of tolrestat (by atom).

A thorough literature survey revealed that our compounds are closely related to the dihydro-1*H*-benzo[*e*]-isoindoles developed by Wrobel and co-workers as conformationally rigid analogues of tolrestat.[28] The author reports that a good inhibitory potency is maintained when the thioamide nitrogen of tolrestat is inserted into a rigid cyclic structure such as a thiolactam ring of five atoms. Such a conformational constraint greatly reduces the flexibility of the molecule, with a beneficial effect on the biological activity.

A preliminary superimposition of NiT **11** on the ALR2-bound conformation of tolrestat shows a satisfactory overlay of the common acetic acid chains and naphthalene rings and of the sulfonyl/thiocarbonyl groups (Figure 1). The match of the fused benzene ring of NiT and the methoxy substituent in position 6 of tolrestat suggests that these moieties might occupy the same lipophilic domain in the enzyme active site. The crystal structure of ALR2 complexed with tolrestat clearly shows that the inhibitor binds at the catalytic site and induces significant conformational changes in a loop (residues 121−135) and a short segment (residues 298−303) to open and fill a contiguous hydrophobic pocket. This so-called "specificity pocket", which is closed in the absence of the inhibitor, is a key determinant for selectivity.[16,29] Thus, our products, with their good superimposition on tolrestat, could be predicted to be more effective against ALR2 than against ALR1.

Moreover, the carbonyl group in position 1 of NiT might theoretically form additional hydrogen bonds with proper amino acid side chains, thus enhancing the inhibitory activity through a better anchoring at the ALR2 catalytic site.

These findings prompted us to synthesize and test for their ALR2 inhibitory activity a number of derivatives in which structural modifications were made in positions 2, 4, 6, and 9 of the naphtho[1,2-*d*]isothiazole

Scheme 1

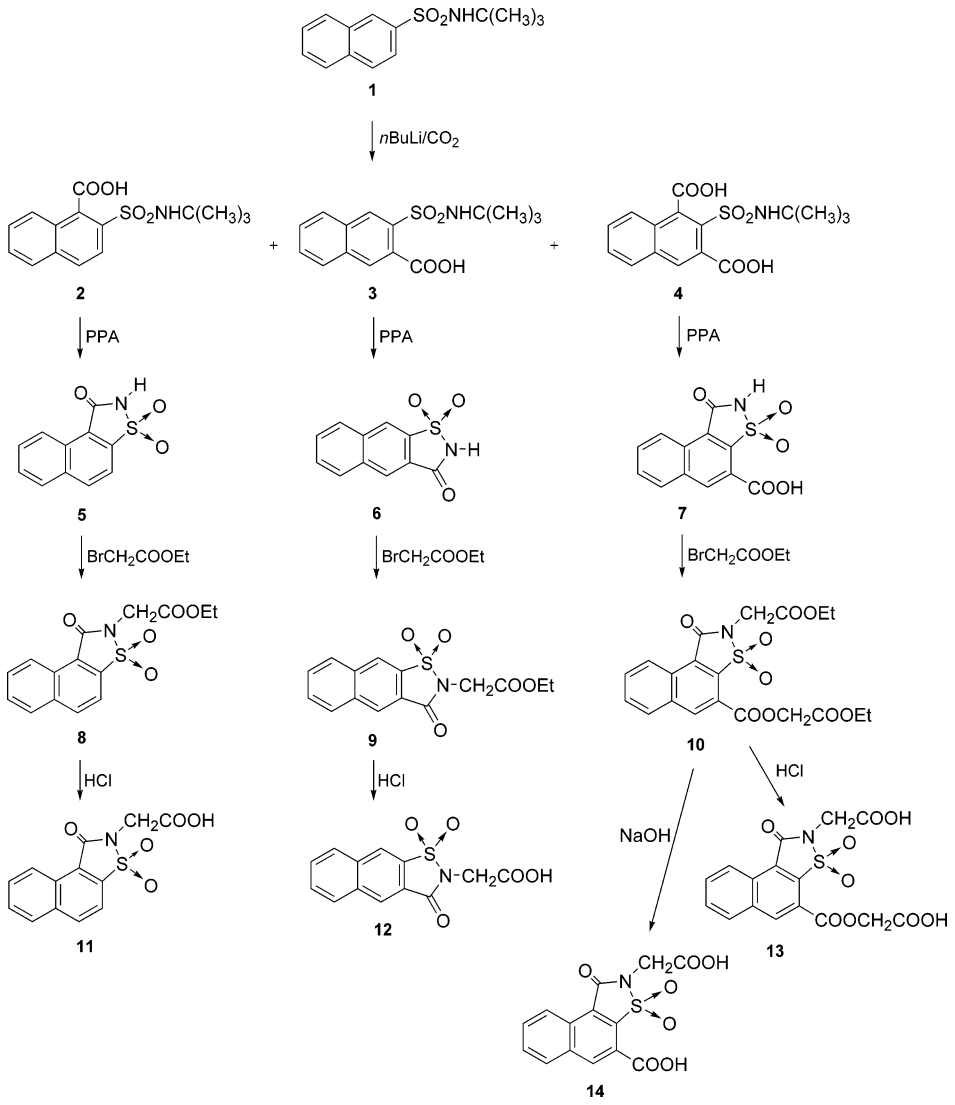

scaffold. To define the structure−activity relationships (SARs) of this class of inhibitors clearly, the acetic acid derivative of linear 3,3-dioxide-1,2-dihydronaphtho[2,3-*d*]isothiazol-1-one **12** was also likewise prepared and tested.

Compound **14**, the most active of the series, and its diisopropyl ester **31** were also investigated in vivo for their ability to prevent cataract development in galactosemic rats.

Finally, docking simulations of **13** and **14** into the human ALR2 binding site were carried out to rationalize the SARs observed and to guide, prospectively, the design of new analogues.

Chemistry

The title compounds were obtained as outlined in Schemes 1−4. The synthesis of the naphthoisothiazole nucleus has previously been described by J. G. Lombardino.[30] The author reported that ortho lithiation, carried out with *n*-butyllithium, and subsequent carbonation with CO_2 of 2-(*N*-*tert*-butyl)naphthalenesulfonamide, **1**, gave the carboxylic acid **2**, which was cyclized and dealkylated in one step by polyphosphoric acid at 100 °C to the desired product **5**.

Following the same conditions as the lithiation−carbonation reaction in our laboratory, a mixture of three products was obtained, which were separated by flash chromatography. The pure compounds were identified by ^{1}H NMR spectral data, proving that the acid **2** was obtained with its regioisomer **3** and with the 1,3-dicarboxylic compound **4** in a 30/10/60 ratio, respectively. Treatment of **2** and **3** with polyphosphoric acid resulted in the corresponding naphthoisothiazoles **5** and **6**. The same reaction, conducted on **4**, gave the 1,3,3-trioxo-1,2-dihydronaphtho[1,2-*d*]isothiazole-4-carboxylic acid **7**; the carboxylic group in position 1 of compound **4** is the only acidic function involved in the reaction of cyclization. Actually, the ^{1}H NMR spectrum of **7** shows the downfield doublet of the deshielded peri proton H_9, which is present in **5** but not in **6**.

Each compound **5**−**7** represents a suitable scaffold for the design and the synthesis of novel potential ALR2 inhibitors, introducing an acetic acid chain (which is essential for the inhibition of the enzyme) in position 2 of the NiT nucleus. Furthermore, derivative **7** possesses an additional acid function in position 4 of the naphthoisothiazole backbone, which might either enhance

Scheme 2

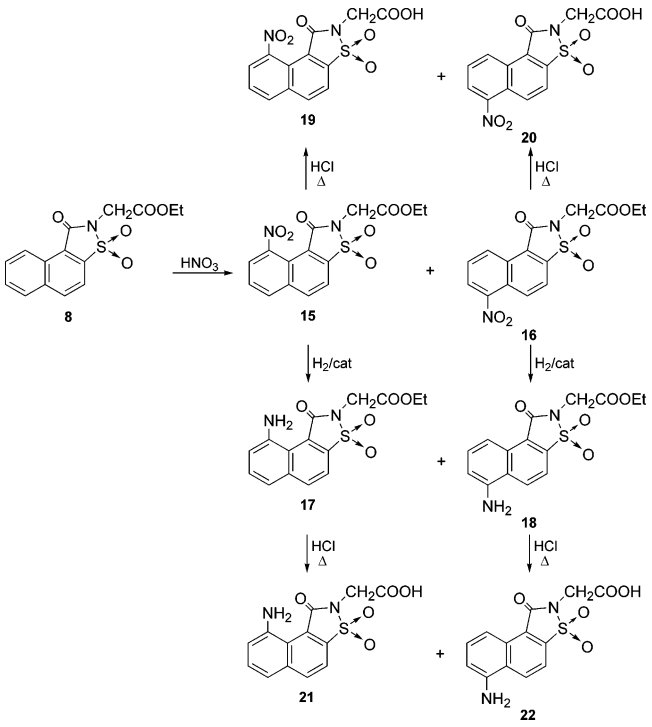

the inhibitory activity or be used to introduce appropriate substituents on the nucleus.

When the sodium salts of **5**−**7** were heated with ethyl bromoacetate in DMF at 100 °C, the ethyl esters **8**−**10** were obtained. Hydrolysis of the isomers **8** and **9** with hot concentrated HCl provided the target acids **11** and **12**. Treatment of **10** with concentrated HCl achieved selective hydrolysis of the ethyl ester groups, and the diacid **13** was the only product of the reaction. Under basic hydrolytic conditions in a water/dioxane solution,[31] the cleavage of all the ester functions was completed and the acid **14** was obtained with a good yield (Scheme 1).

Substitution of positions 6 and 9 of the NiT skeleton with either an electron-withdrawing group, i.e., nitro, or an electron-donating group, i.e., amino, was then performed to verify which type of substituent the fused benzene ring can tolerate (Scheme 2). Thus, by the action of fuming HNO_3 on the ester derivative **8**, the two regioisomers **15** and **16** were obtained, which were separated by flash chromatography and characterized by ^{1}H NMR spectral data. Catalytic hydrogenation of the nitro compounds gave the amino esters **17** and **18**. Finally, hydrolysis of **15**−**18** with hot concentrated HCl gave the desired compounds **19**−**22**.

To test the effective role of the acid residues of **13** and **14** in inhibitor binding and activity, derivatives **25**−**26** and **29**−**30** were also prepared and tested. In these compounds, the *N*-acetic acid moiety was replaced with either a methyl or a benzyl group to verify the effects resulting from changes in residue size and lipophilicity (Scheme 3). Thus, treating the sodium salt of **7** with the appropriate alkyl halide gave the ester derivatives **23** and **24**, which were hydrolyzed in alkaline medium to the corresponding carboxylic acids **25** and **26**. These compounds were then alkylated with ethyl bromoacetate, and the resulting esters **27** and **28** were hydrolyzed with hot concentrated HCl to provide the target products **29** and **30**.

Finally, to improve the ocular bioavailability of acid **14**, the more liphophilic isopropyl diester[32] **31** was prepared and tested.

Results and Discussion

Biological Evaluation. Table 1 lists the inhibitory activities against ALR2 of the tested compounds, expressed as IC_{50} values. As stated in the Introduction, the lead compound **11** showed an appreciable ALR2 inhibitory potency in the micromolar range (10 μM). At first, a new analogue investigation was directed toward the study of the influence on inhibitory potency of substituents with different electronic properties on the benzofused ring in the 6 or 9 positions. Both electron-withdrawing (NO_2) and electron-donating (NH_2) groups determined a detrimental effect on the inhibitory potency with respect to the lead compound **11** (see compounds **19**−**22**); consequently, this type of substitution was no longer investigated.

Because the ALR2 catalytic site is rich in amino acids bearing side chains able to donate or accept hydrogen bonds,[16,29] in principle a second carboxylic group on NiT inhibitors could reinforce the enzyme/inhibitor complex through additional H-bonds.[33] Thus, compound **13** was prepared in which an additional acid group was introduced in position 4 because of its synthetic feasibility. This modification in the molecular structure of **11** gave an 18-fold enhancement in potency (**13** $IC_{50} = 0.55$ μM), thus confirming our design hypothesis. This hypothesis was further confirmed by compound **14**, in which the distance between the additional carboxylic moiety and the molecular nucleus of the inhibitor was shortened, as it showed a gain in inhibitory potency of 2 orders of magnitude with respect to the lead **11** (**14** $IC_{50} = 0.14$ μM).

These results prompted us to verify which of the two carboxylic groups of compounds **13** and **14** was primarily involved in the recognition of the enzyme anionic binding site. In products **25** and **26** and products **29** and **30**, the two different types of carboxylic moieties of **14** and **13**, respectively, were maintained in position 4, whereas the acetic moiety in position 2 was substituted by apolar groups with a different steric hindrance, such as methyl and benzyl. The potencies lower than those of **14** and **13** shown by products **25** and **26** and products **29** and **30** demonstrated that the 2-acetic group is involved in the enzyme pharmacophoric recognition of the inhibitor and that the 4-carboxylic moiety has only an accessory role.

Finally, the shift of the junction between naphthalene and isothiazole from 1,2 to 2,3 to give the linear derivative **12** was totally detrimental for activity. Evidently, only the angular products feature the best spatial relationship among the pharmacophoric groups.

The selected compounds **11**, **13**, **14**, and **26**, when assayed for their ability to inhibit other ALR2-related enzymes, ALR1, SDH, and GR, showed no appreciable inhibitory property, proving them to be completely selective inhibitors of ALR2 (Table 2).

Pharmacological Evaluation of Compounds 14 and 31. Compound **14** was administered as an eyedrop solution in the precorneal region to investigate its in

Scheme 3

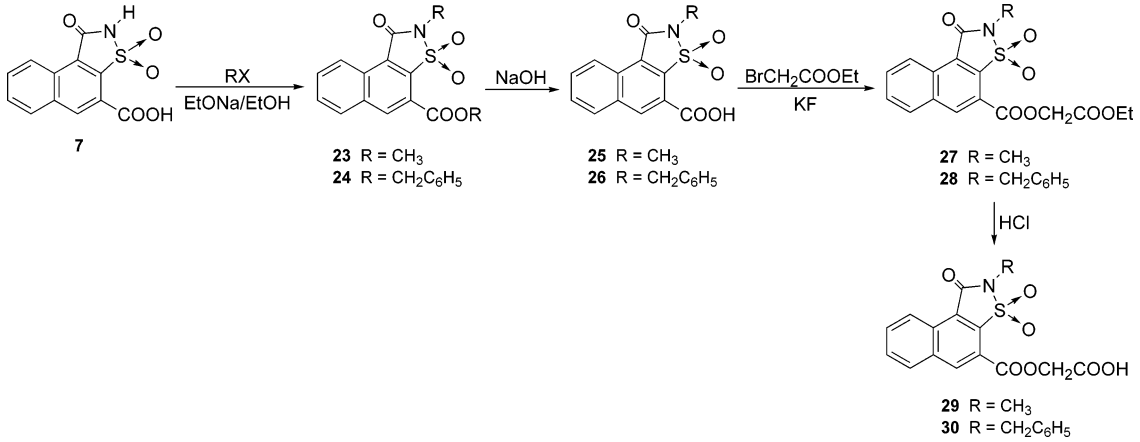

Scheme 4

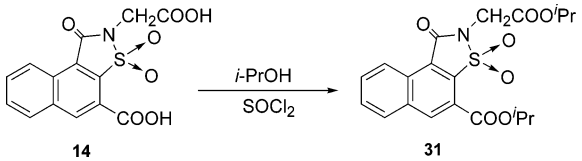

Table 1. ALR2 Inhibition Data of Acid Derivatives **11**−**14**, **19**−**22**, **25**, **26**, **29**, **30**

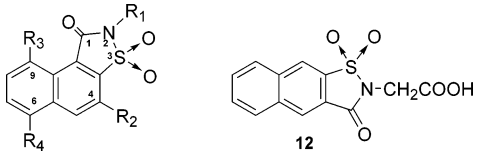

compd	R_1	R_2	R_3	R_4	IC_{50} [a] (μM)
11	CH_2COOH	H	H	H	10 (8.32−11.96)
12					na[b]
13	CH_2COOH	$COOCH_2COOH$	H	H	0.55 (0.49−0.65)
14	CH_2COOH	COOH	H	H	0.14 (0.102−0.155)
19	CH_2COOH	H	NO_2	H	190 (159.8−221.3)
20	CH_2COOH	H	H	NO_2	180 (156.9−209.9)
21	CH_2COOH	H	NH_2	H	100 (87.5−114.7)
22	CH_2COOH	H	H	NH_2	100 (86.7−111.8)
25	CH_3	COOH	H	H	88.0 (72.6−101.2)
26	$CH_2C_6H_5$	COOH	H	H	68.0 (51.5−77.6)
29	CH_3	$COOCH_2COOH$	H	H	na[b]
30	$CH_2C_6H_5$	$COOCH_2COOH$	H	H	100 (91.1−109.3)
tolrestat					0.05 (0.03−0.06)

[a] IC_{50} (95% CL) values represent the concentration required to produce 50% enzyme inhibition. [b] na = not active.

vivo ability to prevent cataract development in severely galactosemic rats. Topical administration can in principle achieve significant drug levels in the lens with negligible effects on other tissues, thus avoiding bioavailability and/or metabolism-related problems associated with systemic administration.[34] It has been reported[35−37] that esters of acid drugs display better corneal permeability and ocular bioavailability by virtue of their higher lipophilicity. Moreover, the employment of an ocular prodrug, which is not active by itself, has the general advantage of being metabolized to its active form only after permeation through the corneal tissue, thus acting only where necessary. Considering that isopropyl esters have shown a good permeability in the corneal tissue,[35] both carboxylic groups of compound **14** were transformed into their isopropyl esters to give **31**, which was tested in vivo as a prodrug. The pharmacological data are reported in Table 3. After 21 days of 50% galactose diet, 90% of the animals treated only with the vehicle developed nuclear cataract. No protection was observed in those treated with 3% ophthalmic solution of acid **14**, whereas rats treated with 3% solution of the isopropyl ester **31** and 1% solution of tolrestat exhibited 55% and 53% protection, respectively. No nuclear cataract was developed by animals administered 3% ophthalmic solution of tolrestat. The potency displayed by prodrug **31** with respect to acid **14** suggests that its higher lipophilicity is essential to permeate the corneal tissue and that its inhibitory activity is ensured by a quick hydrolysis to the active acid by corneal esterases.

Molecular Modeling. To better understand the fairly good ARI inhibitory potency of both compounds **13** and **14** at the molecular level, experiments on docking into the binding pocket of the porcine ALR2/$NADP^+$/tolrestat complex (PDB entry code 1AH3) were performed. Docking experiments were carried out using the automated docking program AutoDock,[38] which allows torsional flexibility in the ligand and incorporates an efficient Lamarckian genetic search algorithm together with an empirical free energy function.

Although the inhibition assays on our compounds were conducted on rat ALR2, the use of the crystal structure of porcine ALR2 for docking studies is justified by the following facts: (i) the crystal structure of rat ALR2 is unknown; (ii) the porcine and rat sequences of this enzyme are characterized by 81% identity and 87% homology;[39] (iii) all active-site residues, including those of the specificity pocket, are largely conserved across the ALR2 isoforms so far sequenced.

The energy-minimized structure of tolrestat was preliminarily docked into ALR2 to examine how closely the AutoDock algorithm can reproduce the experimentally determined binding conformation of tolrestat at the active site of ALR2. The docking test indicated that the largest cluster of similar conformations with the lowest-energy docked structure reproduced very closely the crystallographic binding mode of tolrestat to ALR2. The hydrogen bonds predicted by AutoDock were virtually identical to those found in the crystal structure.

Docking of **13** and **14** to the ALR2 crystal structure revealed a very clear preference for a single position in the active site; the results with the best binding energy (−8.9 and −8.4 kcal/mol) were found 33 and 39 times out of 50, respectively. The ligands were found to be in

Table 2. Enzyme Inhibition Data of Selected Compounds **11**, **13**, **14**, and **26**

compd	aldose reductase IC_{50} [a] (μM)	aldehyde reductase IC_{50} [a] (μM)	sorbitol dehydrogenase IC_{50} [a] (μM)	glutathione reductase IC_{50} [a] (μM)
11	10 (8.32−11.96)	na[b]	na[b]	na[b]
13	0.55 (0.49−0.65)	na[b]	na[b]	na[b]
14	0.14 (0.102−0.155)	na[b]	na[b]	na[b]
26	68.0 (51.5−77.6)	na[b]	na[b]	na[b]
sorbinil	0.65 (0.49−0.82)	0.029 (0.020−0.038)	na[b]	na[b]
tolrestat	0.05 (0.03−0.06)	na[b]	na[b]	na[b]
quercetin	7.81 (5.47−10.15)	2.32 (2.05−2.78)	35.6 (31.6−40.0)	48.8 (34.7−63.4)

[a] IC_{50} values represent the concentration required to produce 50% enzyme inhibition. [b] na = not active.

Table 3. Effects of Treatment with Ophthalmic Solution of **14**, **31**, and Tolrestat on Development of Nuclear Cataract in Severely Galactosemic Rats

	rats with nuclear cataract, %				
day of treatment	control	**14** (3%)	**31** (3%)	tolrestat (1%)	tolrestat (3%)
11	13	0	0	0	0
12	25	0	0	0	0
13	25	13	0	0	0
14	25	15	0	23	0
15	25	25	0	32	0
16	31	25	10	32	0
17	50	25	10	32	0
18	50	25	28	43	0
19	75	50	35	43	0
20	88	85	45	47	0
21	90	90	45	47	0

the same location as tolrestat in the crystal structure. Figure 2 illustrates a selection of residues (4 Å) interacting with the inhibitors in the structure of the minimized complex.

As previously observed in crystal structures of ALR2 complexed with carboxylic acid inhibitors,[15,16,39−41] both analyzed molecules were bound in the active site with their acetic acid moiety entering the anion binding site. Both carboxylic oxygen atoms are within hydrogen-bonding distance of the imidazolium $N^{\epsilon 2}$ atom of His110. Further, the O^{η} hydrogen of Tyr48 and the $N^{\epsilon 1}$ hydrogen of Trp111 form two hydrogen bonds with alternate carboxylic oxygen atoms. The acetic acid substituent is also held in place by numerous van der Waals interactions with the nicotinamide ring of $NADP^+$. Thus, the carboxylate group in position 2 is firmly anchored in the active site, suggesting that it is an essential requirement for the inhibitory activity of these series of compounds. Intriguingly, the couples of compounds **25**/**26** and **29**/**30**, in which the acetic substituent is replaced by a methyl and a benzyl group, respectively, are completely inactive evidently because they lack the acidic substituent able to interact with Tyr48, His110, and Trp111, which are three key residues in binding and catalysis.[42,43]

Moreover, inspection of the **14**/ALR2 complex indicates that the carbonyl oxygen in the 1 position of the isothiazole ring forms a hydrogen bond with the $N^{\epsilon 1}$ hydrogen of Trp111, while one of the two sulfonyl oxygens is positioned to form a weak hydrogen bond with the $N^{\epsilon 1}$ of Trp20, thus contributing to a further stabilization of the complex. By contrast, in the case of inhibitor **13**, it is noted that neither the carbonyl oxygen in the 1 position nor the two sulfonyl oxygens are involved in hydrogen-bonding interactions with Trp111 $N^{\epsilon 1}$ or Trp20 $N^{\epsilon 1}$ hydrogens, respectively, thus explaining the slight difference in activity between **13** (IC_{50} = 0.55 μM) and **14** (IC_{50} = 0.14 μM).

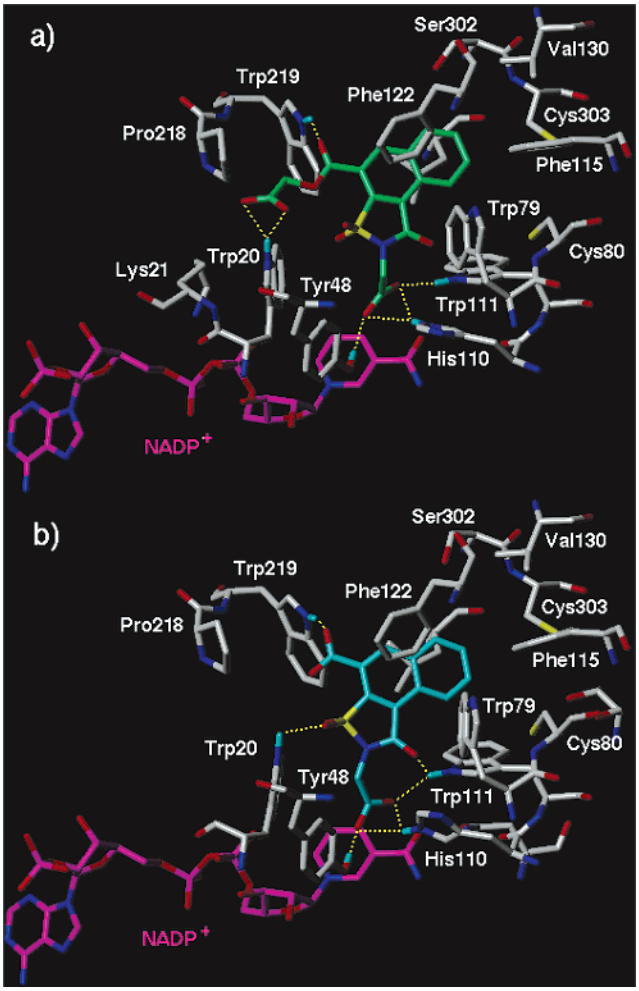

Figure 2. Docked structure of (a) inhibitor **13** (green-blue) and (b) inhibitor **14** (cyan) in the ALR2 active site. Only amino acids located within 4 Å distance of the bound ligand are displayed and labeled. Nonpolar hydrogens have been removed for clarity. $NADP^+$ is shown in magenta. Hydrogen bonds are represented by dashed yellow lines.

In addition, the carboxylate group and the carbonyl oxygen of the ester function in the 4 position of **13** are engaged in hydrogen-bonding interactions with both Trp20 and Trp219 $N^{\epsilon 1}$ hydrogens, respectively. Interestingly, the carboxylate group in the 4 position of inhibitor **14** is also hydrogen-bonded with the $N^{\epsilon 1}$ hydrogen of Trp219, thus providing further evidence of the importance of these additional acidic groups for inhibitor binding to ALR2.

The hydrophobic naphthalene system of both inhibitors gets trapped tightly in a hydrophobic pocket formed

by Trp79, Trp111, Phe115, Phe122, Cys303, and Trp219, making a T-shaped interaction with the Phe122 side chain. The finding that **13** and **14** fit into this pocket, designed as a specificity pocket, has important consequences for the selectivity of inhibitors for ALR2 with respect to ALR1. In fact, these two enzymes differ mainly in the residues composing the hydrophobic pocket, the rest of the enzyme being largely conserved.[16,44] Inhibitors able to bind in this pocket have been reported to be selective for ALR2.[16] The finding that **13** and **14** bind in the hydrophobic pocket accounts for the selectivity observed for these inhibitors.

From the docking model illustrated in Figure 3, it may also be deduced that the low ALR2 inhibitory activity of the 6- or 9-substituted derivatives (compounds **19**−**22**) is a consequence of steric clashes with the walls of the enzyme hydrophobic cleft.

To understand the ALR2 inactivity of **12**, this compound was docked into the ALR2 catalytic site. AutoDock predicted a binding mode associated with a scarcely populated cluster (8/50) and a high estimated ΔG_{bind} (−7,32 kcal/mol). From a visual inspection of the **12**/ALR2 complex, it seems clear that the linear structure of the ligand prevents it from adapting properly into the ALR2 active site, thus not allowing the acetic residue in the 2 position of the ligand to interact favorably with the oxyanion hole made up of His110, Trp111, and Tyr48 residues. This may be the reason for the loss of ALR2 inhibitory activity of **12**.

Experimental Section

Chemistry. Melting points were determined using a Reichert Köfler hot-stage apparatus and are uncorrected. Infrared spectra were recorded with a FT-IR spectrometer Nicolet/Avatar in Nujol mulls. Routine nuclear magnetic resonance spectra were recorded in DMSO-d_6 solution on a Varian Gemini 200 spectrometer operating at 200 MHz. Mass spectra were obtained on a Hewlett-Packard 5988 A spectrometer using a direct injection probe and an electron beam energy of 70 eV. Evaporation was performed in vacuo (rotary evaporator). Analytical TLC was carried out on Merck 0.2 mm precoated silica gel aluminum sheets (60 F-254). Silica gel 60 (230−400 mesh) was used for flash chromatography. Elemental analyses were performed by our Analytical Laboratory and agreed with theoretical values to within ±0.4%. The 2-(*N*-*tert*-butyl)naphthalenesulfonamide **1** was prepared in accordance with a reported procedure.[30]

2-*tert*-Butylsulfamoylnaphthalene-1-carboxylic Acid 2, 3-*tert*-Butylsulfamoylnaphthalene-2-carboxylic Acid 3, and 2-*tert*-Butylsulfamoylnaphthalene-1,3-dicarboxylic Acid, 4. *n*-Butyllithium (1.6 M solution in hexane, 7.12 mL, 11.40 mmol) was added dropwise to an ice-cooled solution of 2-(*N*-*tert*-butyl)naphthalenesulfonamide **1** (1.00 g, 3.80 mmol) in 20 mL of anhydrous THF under a dry nitrogen atmosphere. Once addition was complete, the reaction mixture was left under stirring at room temperature for 2 h, then poured into a suspension of solid carbon dioxide in anhydrous ether. The resulting mixture was diluted with water and acidified with concentrated hydrochloric acid under ice-cooling, then extracted with ether. The combined ether extracts were dried, filtered, and evaporated. The resulting crude product was flash-chromatographed (eluting system: dichloromethane/acetic acid = 9/1) to provide the target compounds **2**−**4**, which were purified by recrystallization.

2: mp 200−203 °C (AcOEt); R_f = 0.42; yield 30%. IR ν cm^{-1}: 3201, 1736, 1716. ^{1}H NMR δ ppm: 1.10 (s, 9H, CH_3), 7.69−8.17 (m, 6H, ArH), 13.70 (bs, 1H, COOH, exc). MS *m/e* (%): 292 (100). Anal. ($C_{15}H_{17}NO_4S$) C, H, N.

3: mp 186−190 °C ($CHCl_3$); R_f = 0.65; yield 10%. IR ν cm^{-1}: 3257, 3073, 1721. ^{1}H NMR δ ppm: 1.16 (s, 9H, CH_3), 7.00−8.63 (m, 6H, ArH), 13.20 (bs 1H, COOH, exc). MS *m/e* (%): 292 (100). Anal. ($C_{15}H_{17}NO_4S$) C, H, N.

4: mp >300 °C (AcOEt); R_f = 0.096; yield 60%. IR ν cm^{-1}: 3446, 3208, 3160, 1711. ^{1}H NMR δ ppm: 1.18 (s, 9H, CH_3), 6.81−8.43 (m, 5H, ArH), 14.00 (bs, 1H, COOH, exc). MS *m/e* (%): [M$^+$] 351 (14), 278 (100). Anal. ($C_{16}H_{17}NO_6S$) C, H, N.

3,3-Dioxidenaphtho[1,2-*d*]isothiazole-1(2*H*)-one 5, 1,1-Dioxidenaphtho[2,3-*d*]isothiazole-3(2*H*)-one 6, and 1,3,3-Trioxo-1,2-dihydronaphtho[1,2-*d*]isothiazole-4-carboxylic Acid 7. A suspension of carboxylic acid **2**, **3**, or **4** (1.00 mmol) in polyphosphoric acid (2.00 g) was heated at 100 °C for 15 min while being stirred with a glass stick. The resulting thick syrup was slowly poured into crushed ice, and the resulting white solid was collected and purified by recrystallization from the appropriate solvent.

5: mp 245−248 °C (AcOEt); yield 30%. IR ν cm^{-1}: 3303, 1736, 1705. ^{1}H NMR δ ppm: 7.83 (t, 1H, H_7), 7.89 (t, 1H, H_8), 8.12 (d, 1H, H_5), 8.24 (d, 1H, H_6), 8.57 (d, 1H, H_4), 9.10 (d, 1H, H_9). MS *m/e* (%): [M$^+$] 233 (63), 126 (100). Anal. ($C_{11}H_7NO_3S$) C, H, N.

6: mp >300 °C (^{i}PrOH); yield 30%. IR ν cm^{-1}: 3207, 1733, 1700. ^{1}H NMR δ ppm: 7.84 (t, 2H, H_6, H_7), 8.28 (t, 1H, H_8), 8.31 (s, 1H, NH, exc), 8.33 (t, 1H,H_5), 8.70 (s, 1H, H_9), 8.83 (s, 1H, H_4). MS *m/e* (%): [M$^+$] 233 (82), 126 (100). Anal. ($C_{11}H_7NO_3S$) C, H, N.

7: mp >300 °C (AcOEt); yield 85%. IR ν cm^{-1}: 3407, 3088, 1717, 1697. ^{1}H NMR δ ppm: 7.90−7.99 (m, 2H, H_7, H_8), 7.95 (s, 1H, NH, exc), 8.42 (d, 1H, H_6), 9.12 (s, 1H, H_5), 9.28 (d, 1H, H_9), 14.02 (bs, 1H, COOH, exc). MS *m/e* (%): [M$^+$] 277 (89), 114 (100). Anal. ($C_{12}H_7NO_5S$) C, H, N.

(1,3,3-Trioxo-1,2-dihydronaphtho[1,2-*d*]isothiazol-2-yl)acetic Acid Ethyl Ester 8, (1,3,3-Trioxo-2,3-dihydronaphtho[2,3-*d*]isothiazol-2-yl)acetic Acid Ethyl Ester 9, and 2-Ethoxycarbonylmethyl-1,3,3-trioxo-1,2-dihydronaphtho[1,2-*d*]isothiazole-4-carboxylic Acid Ethoxycarbonylmethyl Ester 10. The naphthoisothiazole derivative **5**, **6**, or **7** (1.00 mmol) was treated with sodium ethoxide (1.00 mmol for **5** and **6**; 2.00 mmol for **7**) in ethanol solution and then evaporated to dryness. The sodium salt obtained was suspended in 5 mL of DMF, ethyl bromoacetate (1.00 mmol for **5** and **6**; 2.00 mmol for **7**) was added, and the mixture was heated at 120 °C until the disappearance of the starting material (4−8 h, TLC analysis). The reaction mixture was then poured into crushed ice, and the separated solid was collected and purified by recrystallization (Supporting Information, Tables 1 and 3).

General Procedure for the Synthesis of (1,3,3-Trioxo-1,2-dihydronaphtho[1,2-*d*]isothiazol-2-yl)acetic Acid 11, (1,3,3-Trioxo-2,3-dihydronaphtho[2,3-*d*]isothiazol-2-yl)-acetic Acid 12, 2-Carboxymethyl-1,3,3-trioxo-1,2-dihydronaphtho[1,2-*d*]isothiazole-4-carboxylic Acid Carboxymethyl Ester 13, (9-Nitro-1,3,3-trioxo-1,2-dihydronaphtho[1,2-*d*]isothiazol-2-yl)acetic Acid 19, (6-Nitro-1,3,3-trioxo-1,2-dihydronaphtho[1,2-*d*]isothiazol-2-yl)-acetic Acid 20, (9-Amino-1,3,3-trioxo-1,2-dihydronaphtho-[1,2-*d*]isothiazol-2-yl)acetic Acid 21, (6-Amino-1,3,3-trioxo-1,2-dihydronaphtho[1,2-*d*]isothiazol-2-yl)acetic Acid 22, 2-Methyl-1,3,3-trioxo-1,2-dihydronaphtho[1,2-*d*]isothiazole-4-carboxylic Acid 29, and 2-Benzyl-1,3,3-trioxo-1,2-dihydronaphtho[1,2-*d*]isothiazole-4-carboxylic Acid 30. The appropriate ethyl ester **8**−**10**, **15**−**18**, **27**, **28** (1.00 mmol) was suspended in 3 mL of concentrated hydrochloric acid and heated under stirring at 100 °C until hydrolysis was complete (3−12 h, TLC analysis). After cooling at room temperature, the reaction mixture was diluted with water and the precipitated target acid **11**−**13**, **19**−**22**, **29**, or **30** was collected and purified by recrystallization (Supporting Information, Tables 2 and 4).

(9-Nitro-1,3,3-trioxo-1,2-dihydronaphtho[1,2-*d*]isothiazol-2-yl)acetic Acid Ethyl Ester 15 and (6-Nitro-1,3,3-trioxo-1,2-dihydronaphtho[1,2-*d*]isothiazol-2-yl)acetic Acid Ethyl Ester 16. Fuming nitric acid (0.40 mL, 10 mmol) was added dropwise to the ice-cooled ethyl ester **8** (0.319 g, 1.00 mmol). Once addition was complete, the reaction mixture was left under stirring at room temperature for 15 min, then

poured onto crushed ice. The separated yellow solid was collected, dried, and flash-chromatographed (eluting system, ethyl acetate/petroleum ether 60−80 °C = 5/5) to obtain the target isomers **15** and **16**, which were purified by recrystallization (Supporting Information, Tables 1 and 3).

(9-Amino-1,3,3-trioxo-1,2-dihydronaphtho[1,2-*d*]isothiazol-2-yl)acetic Acid Ethyl Ester 17 and (6-Amino-1,3,3-trioxo-1,2-dihydronaphtho[1,2-*d*]isothiazol-2-yl)acetic Acid Ethyl Ester 18. A suspension of the nitro derivative **15** or **16** (0.364 g, 1.00 mmol) and 10% palladium on carbon (0.10 mmol) in 100 mL of absolute ethanol was hydrogenated at atmospheric pressure and room temperature until the uptake of hydrogen was achieved. After filtration of the catalyst, the solvent was evaporated to dryness to give the target compound **17** or **18** as a yellow solid, which was purified by recrystallization (Supporting Information, Tables 1 and 3).

2-Methyl-1,3,3-trioxo-1,2-dihydronaphtho[1,2-*d*]isothiazole-4-carboxylic Acid Methyl Ester 23 and 2-Benzyl-1,3,3-trioxo-1,2-dihydronaphtho[1,2-*d*]isothiazole-4-carboxylic Acid Benzyl Ester 24. The naphthoisothiazole derivative **7** (0.277 g, 1.00 mmol) was treated with 2 equiv of sodium ethoxide in ethanol solution and then evaporated to dryness. The sodium salt obtained was suspended in 5 mL of DMF. Methyl iodide or benzyl bromide (1.20 mmol) was added, and the mixture was heated at 120 °C until the disappearance of the starting material (18−24 h, TLC analysis). The reaction mixture was then poured into crushed ice, and the separated solid was collected and purified by recrystallization (Supporting Information, Tables 1 and 3).

General Procedure for the Synthesis of 2-Carboxymethyl-1,3,3-trioxo-1,2-dihydronaphtho[1,2-*d*]isothiazole-4-carboxylic Acid 14, 2-Methyl-1,3,3-trioxo-1,2-dihydronaphtho[1,2-*d*]isothiazole-4-carboxylic Acid 25, and 2-Benzyl-1,3,3-trioxo-1,2-dihydronaphtho[1,2-*d*]isothiazole-4-carboxylic Acid 26. A suspension of the ester derivative **10**, **23**, or **24** (1.00 mmol) in a mixture of dioxane (20 mL) and 5% NaOH solution (20 mL) was left under stirring at room temperature until the hydrolysis was complete (16−18 h, TLC analysis). The reaction mixture was concentrated in vacuo to half its volume and was then acidified with concentrated hydrochloric acid under ice-cooling. The white solid separated was collected and purified by recrystallization (Supporting Information, Tables 2 and 4).

2-Methyl-1,3,3-trioxo-1,2-dihydronaphtho[1,2-*d*]isothiazole-4-carboxylic Acid Ethoxycarbonyl Methyl Ester 27 and 2-Benzyl-1,3,3-trioxo-1,2-dihydronaphtho[1,2-*d*]isothiazole-4-carboxylic Acid Ethoxycarbonyl Methyl Ester 28. A suspension of the appropriate carboxylic acid **25** or **26** (1.00 mmol), ethyl bromoacetate (0.11 mL, 1.00 mmol), and potassium fluoride (0.058 g, 1.00 mmol) in 5 mL of DMF was heated at 120 °C until the disappearance of the starting material (1−2 h, TLC analysis). The reaction mixture was then poured into crushed ice, and the solid separated was collected and purified by recrystallization (Supporting Information, Tables 1 and 3).

2-Isopropoxycarbonylmethyl-1,3,3-trioxo-1,2-dihydronaphtho[1,2-*d*]isothiazole-4-carboxylic Acid Isopropyl Ester 31. The carboxylic acid **14** (0.335 g, 1.00 mmol) was added to an ice-cooled solution of thionyl chloride (1.18 mL, 2.50 mmol) in 10 mL of isopropyl alcohol, and the reaction mixture was heated under reflux for 12 h. After cooling, the volatiles were removed in vacuo and the crude product thus obtained was purified by recrystallization from ethanol. Mp 132−134 °C; yield 84%. IR ν cm^{-1}: 1726, 1608, 1495, 1220, 1120. ^{1}H NMR δ ppm: 1.26 (d, 6H, CH_3), 1.32 (d, 6H, CH_3), 3.78 (s, 2H, CH_2), 5.02 (m, 1H, CH), 5.20 (m, 1H, CH), 7.60−7.67 (m, 2H, H_7, H_8), 8.03 (d, 1H, H_6), 7.93 (s, 1H, H_5), 8.14 (d, 1H, H_9). MS *m/e* (%): [M$^+$] 419 (14), 143 (100). Anal. ($C_{20}H_{21}NO_7S$) C, H, N.

Biology. Materials and Methods. Aldose reductase (ALR2) and aldehyde reductase (ALR1) were obtained from Sprague Dawley albino rats, 120−140 g body weight, supplied by Harlan Nossan, Italy. To minimize cross-contamination between ALR2 and ALR1 in the enzyme preparation, rat lens (in which ALR2 is the predominant enzyme) and kidney (where ALR1 shows the highest concentration) were used for the isolation of ALR2 and ALR1, respectively.

Glutathione reductase (GR) type IV from baker's yeast (100−300 U/mg), sorbitol dehydrogenase (SDH) from sheep liver (10 U/mg of protein), pyridine coenzymes, D,L-glyceraldehyde, glutathione disulfide, sodium D-glucuronate, sorbitol, and quercetin were from Sigma Chemical Co. Sorbinil was a gift from Pfizer, Groton, CT. Tolrestat was obtained from Lorestat Recordati, Italy. All other chemicals were of reagent grade.

Enzyme Preparation. Aldose Reductase (ALR2). A purified rat lens extract was prepared in accordance with the method of Hayman and Kinoshita[45] with slight modifications. Lenses were quickly removed from rats following euthanasia and were homogenized (Glas-Potter) in 3 volumes of cold deionized water. The homogenate was centrifuged at 12 000 rpm at 0−4 °C for 30 min. Saturated ammonium sulfate solution was added to the supernatant fraction to form a 40% solution, which was stirred for 30 min at 0−4 °C and then centrifuged at 12 000 rpm for 15 min. Following this same procedure, the recovered supernatant was subsequently fractionated with saturated ammonium sulfate solution using first a 50% and then a 75% salt saturation. The precipitate that was recovered from the 75% saturated fraction, possessing ALR2 activity, was redissolved in 0.05 M NaCl and dialyzed overnight in 0.05 M NaCl. The dialyzed material was used for the enzymatic assay.

Aldehyde Reductase (ALR1). Rat kidney ALR1 was prepared in accordance with a previously reported method.[46] Kidneys were quickly removed from normal killed rats and homogenized (Glas-Potter) in 3 volumes of 10 mM sodium phosphate buffer, pH 7.2, containing 0.25 M sucrose, 2.0 mM EDTA dipotassium salt, and 2,5 mM β-mercaptoethanol. The homogenate was centrifuged at 12 000 rpm at 0−4 °C for 30 min, and the supernatant was subjected to a 40−75% ammonium sulfate fractionation, following the same procedure previously described for ALR2. The precipitate obtained from the 75% ammonium sulfate saturation, possessing ALR1 activity, was redissolved in 50 volumes of 10 mM sodium phosphate buffer, pH 7.2, containing 2.0 mM EDTA dipotassium salt and 2.0 mM β-mercaptoethanol and was dialyzed overnight using the same buffer. The dialyzed material was used in the enzymatic assay.

Enzymatic Assays. The activity of the four test enzymes was determined spectrophotometrically by monitoring the change in absorbance at 340 nm, which is due to the oxidation of NADPH or the reduction of NAD$^+$ catalyzed by ALR2, ALR1, and GR or SDH, respectively. The change in pyridine coenzyme concentration per minute was determined using a Beckman DU-64 kinetics software program (Solf Pack TM module).

ALR2 activity was assayed at 30 °C in a reaction mixture containing 0.25 mL of 10 mM d,L-glyceraldehyde, 0.25 mL of 0.104 mM NADPH, 0.25 mL of 0.1 M sodium phosphate buffer (pH 6.2), 0.1 mL of enzyme extract, and 0.15 mL of deionized water in a total volume of 1 mL. All the above reagents, except D,L-glyceraldehyde, were incubated at 30 °C for 10 min. The substrate was then added to start the reaction, which was monitored for 5 min. Enzyme activity was calibrated by diluting the enzymatic solution in order to obtain an average reaction rate of 0.011 ± 0.0010 absorbance units/min for the sample.

ALR1 activity was determined at 37 °C in a reaction mixture containing 0.25 mL of 20 mM sodium D-glucuronate, 0.25 mL of 0.12 mM NADPH, 0.25 mL of dialyzed enzymatic solution, and 0.25 mL of 0.1 M sodium phosphate buffer (pH 7.2) in a total volume of 1 mL. The enzyme activity was calibrated by diluting the dialyzed enzymatic solution in order to obtain an average reaction rate of 0.015 ± 0.0010 absorbance units/min for the sample.

SDH activity[47] was determined at 37 °C in a reaction mixture containing 0.25 mL of 10 mM sorbitol, 0.25 mL of 0.47 mM NAD$^+$, 0.25 mL of 3.75 mU/mL enzymatic solution, and 0.25 mL of 100 mM Tris-HCl buffer (pH 8) in a total volume

of 1 mL. All the reagents were incubated at 37 °C for 1 min, after which the reaction was monitored for 3 min.

GR activity[48] was determined at 37 °C in a mixture containing 0.25 mL of 1 mM glutathione disulfide, 0.25 mL of 0.36 mM NADPH, 0.25 mL of 4.5 mU/mL enzymatic solution, and 0.25 mL of 0.125 sodium phosphate buffer (pH 7.4) supplemented with 6.3 mM EDTA potassium salt, in a total volume of 1 mL.

Enzymatic Inhibition. The inhibitory activity of the newly synthesized compounds against ALR2, ALR1, SDH, and GR was assayed by adding 0.1 mL of the inhibitor solution to the reaction mixture described above. All the inhibitors were solubilized in water, and the solubility was facilitated by adjustment to a favorable pH. After solubilization was complete, the pH was readjusted to 7. To correct for the nonenzymatic oxidation of NADPH or reduction of NAD^+ and for the absorption by the compounds tested, a reference blank containing all the above assay components except the substrate was prepared. The inhibitory effect of the new derivatives was routinely estimated at a concentration of 10^{-4} M. Those compounds found to be active were tested at additional concentrations between 10^{-5} and 10^{-7} M. The determination of the IC_{50} values was performed by using linear regression analysis of the log dose response curve, which was generated using at least four concentrations of the inhibitor causing an inhibition between 20% and 80%, with two replicates at each concentration. The 95% confidence limits (95% CL) were calculated from t values for $n - 2$, where n is the total number of determinations.

Pharmacology. Materials and Methods. Experiments were carried out using Sprague Dawley albino rats, 45−55 g body weight, supplied by Harlan-Nossan, Italy. Animal care and treatment conformed to the ARVO Resolution on the Use of Animals in Ophthalmic and Vision Research. The galactose diet consisted of a pulverized mixture of 50% D-galactose and 50% TRM laboratory chow (Harlan Teckland U.K.), and the control diet consisted of normal TRM. Both control and experimental rats had access to food and water ad libitum.

Prevention of Cataract Development. Animals were randomly divided into groups of equal average body weight with 15 rats per group. The test compounds **14**, **31**, and tolrestat were administered four times daily as eye drops of appropriate concentrations. The vehicle in which ARIs were contained was administered with the same dose regimen to the control group, which was given access to the galactose diet, and to the group fed with a normal diet, which was included to record the aspect of normal lenses. Groups treated with the tested compounds were predosed 1 day before switching their diet to galactose-containing chow.

Lenses were examined using slit-lamp microscopy after dilating the pupils with 1% atropine, Farmigea, Italy, to establish their integrity.

Nuclear cataracts, which appeared as a pronounced central opacity readily visible as a white spot, were evaluated. The number of animals that attained this stage was recorded, and the ability of the test compounds to prevent cataract development was assessed on the basis of comparison with galactosemic rats treated only with the vehicle.

Computational Chemistry. Molecular modeling and graphics manipulations were performed using the SYBYL software package[49] running on a Silicon Graphics R12000 workstation. Model building of inhibitors **11**−**14** was accomplished with the Tripos force field[50] available within SYBYL. Energy minimizations of the inhibitor/ALR2 complexes were carried out by employing the Insight II/Discover program,[51] selecting the CVFF force field.[52]

Docking Simulations. Docking was performed with version 3.05 of the program AutoDock.[38] It combines a rapid energy evaluation through precalculated grids of affinity potentials with a variety of search algorithms to find suitable binding positions for a ligand on a given protein. While the protein is required to be rigid, the program allows torsional flexibility in the ligand.

Docking to ALR2 was carried out using the empirical free energy function and the Lamarckian genetic algorithm, applying a standard protocol with an initial population of 50 randomly placed individuals, a maximum number of 1.5×10^6 energy evaluations, a mutation rate of 0.02, a crossover rate of 0.80, and an elitism value of 1. Proportional selection was used, where the average of the worst energy was calculated over a window of the previous 10 generations. For the local search, the so-called pseudo Solis and Wets algorithm was applied using a maximum of 300 iterations per local search. The probability of performing local search on an individual in the population was 0.06, and the maximum number of consecutive successes or failures before doubling or halving the local search step size was 4.

Fifty independent docking runs were carried out for each ligand. Results differing by less than 1.5 Å in positional root mean-square deviation (rmsd) were clustered together and represented by the result with the most favorable free energy of binding.

Ligand Setup. Molecular models of compounds **11**−**14** were constructed using standard bond lengths and bond angles of the SYBYL fragment library. The carboxylate group was taken as dissociated. Geometry optimizations were carried out with the SYBYL/MAXIMIN2 minimizer by applying the BFGS (Broyden, Fletcher, Goldfarb, and Shannon) algorithm[53] and setting an rms gradient of the forces acting on each atom of 0.05 kcal mol^{-1} $Å^{-1}$ as the convergence criterion.

Atomic charges were assigned using the Gasteiger−Marsili formalism,[54] which is the type of atomic charge used in calibrating the AutoDock empirical free energy function. Finally, the compounds were set up for docking with the help of AutoTors, the main purpose of which is to define the torsional degrees of freedom to be considered during the docking process. The number of flexible torsions defined for each ligand is as follows: 2 in **11**, 2 in **12**, 5 in **13**, and 3 in **14**.

Protein Setup. The crystal structure of ALR2 complexed with tolrestat (entry code: 1AH3),[16] recovered from Brookhaven Protein Database,[55] was used. The structure was set up for docking as follows: polar hydrogens were added using the PROTONATE utility.[38] To optimize the hydrogen positions, the structure was subjected to a short energy minimization using the Discover module of InsightII, in accordance with the type of force field and protein charges of the AutoDock empirical free energy function. Solvation parameters were added to the final protein file using the ADDSOL utility of AutoDock3.5.

The grid maps representing the proteins in the actual docking process were calculated with AutoGrid. The grids (one for each atom type in the ligand plus one for electrostatic interactions) were chosen to be sufficiently large to include not only the active site but also significant portions of the surrounding surface. The dimensions of the grids were thus 30 Å × 30 Å × 30 Å, with a spacing of 0.375 Å between the grid points.

Refinement of the inhibitor/enzyme complexes was achieved by energy minimization with the CVFF force field, permitting only the ligand and the side chain atoms of the protein to relax. Calculations were performed by using 3000 steps of steepest descents and 2000 steps of conjugate gradients (down to a maximal atomic root-mean-square derivative of 10.0 and 0.01 kcal/Å, respectively).

Supporting Information Available: Tables 1−4 including physical and spectral data of compounds **8**−**30** and analytical data of compounds **2**−**31**. This material is available free of charge via the Internet at http://pubs.acs.org.

References

(1) King, H.; Aubert, R. E.; Herman, W. H. Global Burden of Diabetes, 1995−2025. Prevalence, Numeric Estimates, and Projections. *Diabetes Care* **1998**, *21*, 1414−1431.
(2) Bressler, R.; Johnson, D. New Pharmacological Approaches to Therapy of NIDDM. *Diabetes Care* **1992**, *15*, 792−805.

(3) Mahon, J. L.; Dupre, J.; Stiller, C. R. Lessons Learned from Use of Cyclosporine for Insulin-Dependent Diabetes Mellitus. The Case of Immunotherapy for Insulin-Dependent Diabetics Having Residual Insulin Secretion. *Ann. N.Y. Acad. Sci*. **1993**, *696*, 3651−3663.
(4) Brownlee, M. Biochemistry and Molecular Cell Biology of Diabetic Complications. *Nature* **2001**, *414*, 813−820.
(5) Scott, J. A.; King, G. L. Oxidative Stress and Antioxidant Treatment in Diabetes. *Ann. N.Y. Acad. Sci.* **2004**, *1031*, 204−213.
(6) Whiteside, C. I. Cellular Mechanisms and Treatment of Diabetes Vascular Complications Converge on Reactive Oxygen Species. *Curr. Hypertens. Rep*. **2005**, *7*, 148−154.
(7) Brownlee, M. The Pathological Implications of Protein Glycation. *Clin. Invest. Med*. **1995**, *18*, 275−281.
(8) Tomlinson, D. R.; Stevens, E. J.; Diemel, L. T. Aldose Reductase Inhibitors and Their Potential for the Treatment of Diabetic Complications. *Trends Pharmacol. Sci.* **1994**, *15*, 293−297.
(9) Kador, P. F. The Role of Aldose Reductase in the Development of Diabetic Complications. *Med. Res. Rev.* **1988**, *8*, 325−352.
(10) Bravi, M. C.; Pietrangeli, P.; Laurenti, O.; Basili, S.; Cassone-Faldetta, M.; Ferri, C.; De Mattia, C. Polyol Pathway Activation and Glutathione Redox Status in Non-Insulin-Dependent Diabetic Patients. *Metabolism* **1997**, *46*, 1194−1198.
(11) Cheng, H. M.; Gonzales, R. G. The Effect of High Glucose and Oxidative Stress on Lens Metabolism, Aldose Reductase, and Senile Cataractogenesis. *Metabolism* **1986**, *35*, 10−14.
(12) Chung, S. S. M.; Ho, E. C. M.; Lam, K. S. L.; Chung, S. K. Contribution of Polyol Pathway to Diabetes-Induced Oxidative Stress. *J. Am. Soc. Nephrol*. **2003**, *14*, S234−S236.
(13) Morre, D. M.; Lenaz, G.; Morre, D. J. Surface Oxidase and Oxidative Stress Propagation in Aging. *J. Exp. Biol*. **2000**, *203*, 1513−1521.
(14) Sarges, R.; Oates, P. J. Aldose Reductase Inhibitors: Recent Developments. *Prog. Drug Res*. **1993**, *40*, 99−161.
(15) Wilson, D. K.; Tarle, I.; Petrash, J. M.; Quiocho, F. A. Refined 1.8 Å Structure of Human Aldose Reductase Complexed with the Potent Inhibitor Zopolrestat. *Proc. Natl. Acad. Sci. U.S.A.* **1993**, *90*, 9847−9851.
(16) Urzhumtsev, A.; Tête-Favier, F.; Mitschler, A.; Barbanton, J.; Barth, P.; Urzhumtseva, L.; Biellmann, J.-F.; Podjarny, A. D.; Moras, D. A "Specificity" Pocket Inferred from the Crystal Structures of the Complexes of Aldose Reductase with the Pharmaceutically Important Inhibitors Tolrestat and Sorbinil. *Structure* **1997**, *5*, 601−612.
(17) Harrison, D. H. T.; Bohren, K. M.; Petsko, G. A.; Ringe, D.; Gabbay, K. H. The Alrestatin Double-Decker: Binding of Two Inhibitor Molecules to Human Aldose Reductase Reveals a New Specificity Determinant. *Biochemistry* **1997**, *36*, 16134−16140.
(18) Harrison, D. H.; Bohren, K. M.; Ringe, D.; Petsko, G. A.; Gabbay, K. H. An Anionic Binding Site in Human Aldose Reductase: Mechanistic Implications for the Binding of Citrate, Cacodylate, and Glucose-6-phosphate. *Biochemistry* **1994**, *33*, 2011−2020.
(19) Carper, D.; Wistow, G.; Nishimura, C.; Graham, C.; Watanabe, K.; Fuji, Y.; Hayaishi, H.; Hayaishi, O. A Superfamily of NADPH-Dependent Reductases in Eukaryotes and Prokaryotes. *Exp. Eye Res*. **1988**, *49*, 377−388.
(20) Costantino, L.; Rastelli, G.; Vescovini, K.; Cignarella, G.; Vianello, P.; Del Corso, A.; Cappiello, M.; Mura, U.; Barlocco, D. Synthesis, Activity, and Molecular Modeling of a New Series of Tricyclic Pyridazinones as Selective Aldose Reductase Inhibitors. *J. Med. Chem.* **1996**, *39*, 4396−4405.
(21) Kador, P. F.; Inoue, J.; Secchi, E. F.; Lizak, M. J.; Rodriguez, L.; Mori, K.; Greentree, W.; Blessing, K.; Lackner, P. A.; Sato, S. Effect of Sorbitol Dehydrogenase Inhibition on Sugar Cataract Formation in Galactose-Fed and Diabetic Rats. *Exp. Eye Res*. **1998**, *67*, 203−208.
(22) Giblin, F. J.; McCready, J. P.; Schrimscher, L.; Reddy, V. N. Peroxide-Induced Effects on Lens Cation Transport Following Inhibition of Glutathione Reductase Activity in Vitro. *Exp. Eye Res.* **1987**, *45*, 77−91.
(23) Reddan, J. R.; Giblin, F. J.; Dziedzic, D. C.; McCready, J. P.; Schrimscher, L.; Reddy, V. N. Influence of the Activity of Glutathione Reductase on the Response of Cultured Lens Epithelial Cells from Young and Old Rabbits to Hydrogen Peroxide. *Exp. Eye Res.* **1998**, *46*, 209−221.
(24) Da Settimo, F.; Primofiore, G.; Da Settimo, A.; La Motta, C.; Taliani, S.; Simorini, F.; Novellino, E.; Greco, G.; Lavecchia, A.; Boldrini, E. [1,2,4]Triazino[4,3-*a*]benzimidazole Acetic Acid Derivatives: A New Class of Selective Aldose Reductase Inhibitors. *J. Med. Chem*. **2001**, *44*, 4359−4369.
(25) Da Settimo, F.; Primofiore, G.; Da Settimo, A.; La Motta, C.; Simorini, F.; Novellino, E.; Greco, G.; Lavecchia, A.; Boldrini, E. Novel, Highly Potent Aldose Reductase Inhibitors: Cyano-(2-oxo-2,3-dihydroindol-3-yl)acetic Acid Derivatives. *J. Med. Chem*. **2003**, *46*, 1419−1428.
(26) Da Settimo, A.; Primofiore, G.; La Motta, C.; Da Settimo, F.; Simorini, F.; Boldrini, E.; Bianchini, P. Acid Derivatives of Benzisothiazole-1,1-dioxide as Inhibitors of Rat Lens Aldose Reductase. *Farmaco* **1996**, *51*, 261−267.
(27) Primofiore, G.; Da Settimo, F.; La Motta, C.; Simorini, F.; Minutolo, A.; Boldrini, E. Benzisothiazole-1,1-dioxide Alkanoic Acid Derivatives as Inhibitors of Rat Lens Aldose Reductase. *Farmaco* **1997**, *52*, 583−588.
(28) Wrobel, J.; Dietrich, A.; Gorham, B. J.; Sestanj, K. Conformationally Rigid Analogues of Aldose Reductase Inhibitors, Tolrestat. Novel Syntheses of Naphthalene-Fused γ-, δ-, and ϵ-Lactams. *J. Org. Chem*. **1990**, *55*, 2694−2702.
(29) El-Kabbani, O.; Wilson, D. K.; Petrash, J. M.; Quiocho, F. A. Structural Features of the Aldose Reductase and Aldehyde Reductase Inhibitor-Binding Sites. *Mol. Vision* **1998**, *4*, 19−25.
(30) Lombardino, J. G. Preparation of Substituted 1,2-Benzoisothiazolin-3-one-1,1-dioxides (*o*-Benzoic Sulfimides). *J. Org. Chem*. **1971** *36*, 1843−1845.
(31) Nicolaou, I.; Demopoulos, V. J. Substituted Pyrrol-1-ylacetic Acids That Combine Aldose Reductase Enzyme Inhibitory Activity and Ability To Prevent the Nonenzymatic Irreversible Modification of Proteins from Monosaccharides. *J. Med. Chem*. **2003**, *46*, 417−426.
(32) Boissonnas, R. A.; Guttmann, St.; Jaquenoud, P.-A.; Waller, J.-P. Synthèse d'Analogues Structuraux de L'oxytocine (Synthesis of Structural Analogues of Oxytocin). *Helv. Chim. Acta* **1956**, *39*, 1421−1427.
(33) Coudert, P.; Albuisson, E.; Boire, J. Y.; Durox, E.; Bastide, P.; Couquelet, J. Synthesis of Pyridazine Acetic Acid Derivatives Possessing Aldose Reductase Inhibitory Activity and Antioxidant Properties. *Eur. J. Med. Chem*. **1994**, *29*, 471−477.
(34) Banditelli, S.; Boldrini, E.; Vilardo, G. P.; Cecconi, I.; Cappiello, M.; Dal Monte, M.; Marini, I.; Del Corso, A.; Mura, U. A New Approach against Sugar Cataract through Aldose Reductase Inhibitors. *Exp. Eye* Res. **1999**, *69*, 533−538.
(35) Camber, O.; Edman, P. Factors Influencing the Corneal Permeability of Prostaglandin $F_{2\alpha}$ and Its Isopropyl Ester in Vitro. *Int. J. Pharm.* **1987**, *37*, 27−32.
(36) Suhonen, P.; Järvinen, T.; Peura, P.; Urtti, A. Permeability of Pilocarpic Acid Diesters across Albino Rabbit Cornea in Vitro. *Int. J. Pharm*. **1991**, *74*, 221−228.
(37) Chien, D.-S.; Tang-Liu, D. D.-S.; Woodward, D. F. Ocular Penetration and Bioconversion of Prostaglandin $F_{2\alpha}$ Prodrugs in Rabbit Cornea and Conjunctiva. *J. Pharm. Sci.* **1997**, *86*, 1180−1186.
(38) Morris, G. M.; Goodsell, D. S.; Halliday, R. S.; Huey, R.; Hart, W. E.; Belew, R. K.; Olson, A. J. Automated Docking Using a Lamarckian Genetic Algorithm and an Empirical Binding Free Energy Function. *J. Comput. Chem.* **1998**, *19*, 1639−1662.
(39) Database searching (SWISS-PROT), sequence alignment, and analysis of rat and pig ALR2 sequences were carried out using FASTA (Pearson, W. R. *Proc. Natl. Acad. Sci. U.S.A.* **1988**, *85*, 2444−2448) and BLAST programs (Wang, S.; Pak, Y. *J. Phys. Chem. B* **2000**, *104*, 354−359). The SWISS-PROT accession numbers for rat and pig ALR2 types are P07943 and P80276, respectively.
(40) Harrison, D. H. T.; Bohren, K. M.; Petsko, G. A.; Ringe, D.; Gabbay, K. H. The Alrestatin Double-Decker: Binding of Two Inhibitor Molecules to Human Aldose Reductase Reveals a New Specificity Determinant. *Biochemistry* **1997**, *36*, 16134−16140.
(41) Rogniaux, H.; Van Dorsselaer, A.; Barth, P.; Biellmann, J.-F.; Barbanton, J.; Van Zandt, M.; Chevrier, B.; Howard, E.; Mitschler, A.; Potier, N.; Urzhumtseva, L.; Moras, D.; Podjarny, A. Binding of Aldose Reductase Inhibitors: Correlation of Crystallographic and Mass Spectrometric Studies. *J. Am. Soc. Mass Spectrom.* **1999**, *10*, 635−647.
(42) Bohren, K. M.; Grimshaw, C. E.; Lai, C. J.; Harrison, D. H.; Ringe, D.; Petsko, G. A.; Gabbay, K. H. Tyrosine-48 Is the Proton Donor and Histidine-110 Directs Substrate Stereochemical Selectivity in the Reduction Reaction of Human Aldose Reductase: Enzyme Kinetics and Crystal Structure of the Y48H Mutant Enzyme. *Biochemistry* **1994**, *33*, 2021−2032.
(43) Grimshaw, C. E.; Bohren, K. M.; Lai, C. J.; Gabbay, K. H. Human Aldose Reductase: p*K* of Tyrosine 48 Reveals the Preferred Ionization State for Catalysis and Inhibition. *Biochemistry* **1995**, *34*, 14374−14384
(44) El-Kabbani, O.; Carper, D. A.; McGowan, M. H.; Devedjiev, Y.; Milton, K. J.; Flynn, T. G. Studies on the Inhibitor-Binding Site of Porcine Aldehyde Reductase: Crystal Structure of the Holoenzyme−Inhibitor Ternary Complex. *Proteins* **1997**, *28*, 186−192.
(45) Hayman, S.; Kinoshita, J. H. Isolation and Properties of Lens Aldose Reductase. *J. Biol. Chem*. **1965**, *240*, 877−882.
(46) Ward, W. H. J.; Sennitt, C. M.; Ross, H.; Dingle, A.; Timmus, D.; Mirrless, D. J.; Tuffin, D. P. Ponalrestat, a Potent and

Specific Inhibitor of Aldose Reductase. *Biochem. Pharmacol*. **1990**, *39*, 337−346.
(47) Lindstad, R. I.; Hermansen, L. F.; McKinley-McKee, J. S. Inhibition and activation studies on sheep liver sorbitol dehydrogenase. *Eur. J. Biochem*. **1994**, *221*, 847−854.
(48) Fitzgerald, G. B.; Bauman, C.; Sajjat Hussoin, Md.; Wick, M. M. 2,4-Dihydroxy benzylamine: a specific inhibitor of glutathione reductase. *Biochem. Pharmacol*. **1991**, *41*, 185−190.
(49) *SYBYL Molecular Modelling System*, version 6.9.1; Tripos Inc.: St. Louis, MO, 2003.
(50) Vinter, J. G.; Davis, A.; Saunders, M. R. Strategic Approaches to Drug Design. 1. An Integrated Software Framework for Molecular Modelling. *J. Comput.-Aided Mol. Des.* **1987**, *1*, 31−55.
(51) *Insight II Molecular Modelling Package* and *Discover 2. 2000 Simulation Package*; MSI Inc.: San Diego, CA, 2000.
(52) Hagler, A. F.; Lifson, S.; Dauber, P. Consistent Force Field Studies of Intermolecular Forces in Hydrogen-Bonded Crystals. *J. Am. Chem. Soc.* **1979**, *101*, 5122−5130.
(53) Head, J.; Zerner, M. C. A Broyden−Fletcher−Goldfarb−Shannon Optimization Procedure for Molecular Geometries. *Chem. Phys. Lett.* **1985**, *122*, 264−274.
(54) Gasteiger, J.; Marsili, M. Iterative Partial Equalization of Orbital Electronegativity. A Rapid Access to Atomic Charges. *Tetrahedron* **1980**, *36*, 3219−3228.
(55) Bernstein, F. C.; Koetzle, T. F.; Williams, G. J. B.; Meyer, E. F., Jr.; Brice, M. D.; Rodgers, J. R.; Kennard, O.; Shimanouchi, T.; Tasumi, T. The Protein Data Bank: A Computer Based Archival File for Macromolecular Structures. *J. Mol. Biol.* **1977**, *112*, 535−542.

JM050382P